

Demonstration of a semipolar ($10\bar{1}\bar{3}$) InGaN/GaN green light emitting diode

R. Sharma,^{a)} P. M. Pattison, and H. Masui

Materials Department, University of California, Santa Barbara, California 93106

R. M. Farrell

Electrical and Computer Engineering Department, University of California, Santa Barbara, California 93106

T. J. Baker, B. A. Haskell, F. Wu, S. P. DenBaars, J. S. Speck, and S. Nakamura

NICP/ERATO JST, UCSB Group, and Materials Department, University of California, Santa Barbara, California 93106

(Received 20 June 2005; accepted 11 October 2005; published online 30 November 2005)

We demonstrate the growth and fabrication of a semipolar ($10\bar{1}\bar{3}$) InGaN/GaN green (~ 525 nm) light emitting diode (LED). The fabricated devices demonstrated a low turn-on voltage of 3.2 V and a series resistance of 14.3 Ω . Electroluminescence measurements on the semipolar LED yielded a reduced blueshifting of the peak emission wavelength with increasing drive current, compared to a reference commercial *c*-plane LED. On-wafer measurements yielded an approximately linear increase in output power with drive current, with measured values of 19.3 and 264 μ W at drive currents of 20 and 250 mA, respectively. The external quantum efficiency did not decrease appreciably at high currents. Polarization anisotropy was also observed in the electroluminescence from the semipolar green LED, with the strongest emission intensity parallel to the $[1\bar{2}10]$ direction. A polarization ratio of 0.32 was obtained at a drive current of 20 mA. © 2005 American Institute of Physics. [DOI: 10.1063/1.2139841]

Current commercially available III-nitride based optoelectronic devices typically consist of epitaxial multilayer thin films grown along the polar *c* direction of the wurtzite crystal structure. The performance of these devices suffers from strong polarization-induced electric fields along the polar *c* direction, which results in reduced overlap between the electron and hole wave functions in the quantum wells.^{1–4} As a result, these devices typically demonstrate a low radiative recombination rate, as well as a blueshift in peak emission wavelength with increasing bias due to the carrier-induced screening of the polarization-induced electric fields. Additionally, the density of states in the valence band is much higher than the density of states in the conduction band in these structures,⁵ and as a result, very high carrier densities are needed to generate optical gain.

Recently, there have been several reports of light emitting diodes (LEDs) fabricated on nonpolar *a*- and *m*-plane GaN.^{6–9} These devices show a negligible to zero blueshift of peak emission wavelength with increasing drive currents, indicative of the expected absence of polarization-induced electric fields along the conduction direction. Additionally, theoretical results suggest that the effective hole mass in strained nonpolar InGaN quantum wells is smaller than that in strained *c*-plane InGaN quantum wells.¹⁰ Recent work on nonpolar *m*-plane films grown by molecular beam epitaxy¹¹ has yielded hole concentrations that are almost an order of magnitude higher than for *c*-plane films.

Another approach to decreasing or potentially eliminating the polarization effects and reducing effective hole masses is to grow nitride heterostructures on so-called “semipolar” planes, i.e., upon planes that may not be classified as

c, *a*, or *m* planes, and have at least two nonzero *h*, *i*, or *k* Miller indices and a nonzero ℓ Miller index. By extension, it is expected that nitride-based LEDs wherein the conduction direction is along semipolar directions (parallel to the plane normals of $\{10\bar{1}1\}$, $\{10\bar{1}2\}$, and $\{10\bar{1}3\}$ planes, for instance) should demonstrate behavior indicative of reduced polarization-induced electric fields¹² and higher hole concentrations,¹⁰ when compared with devices in which the conduction direction is along the polar *c* direction. The semipolar planes are believed to be stable over a wide range of growth conditions,^{13,14} unlike nitride growth on nonpolar planes. Furthermore, the indium incorporation efficiency for semipolar growth is believed to be comparable to that observed in *c*-plane growth, and it is predicted that for particular semipolar planes, the value of piezoelectric polarization will approach zero at specific indium compositions in compressively strained InGaN quantum wells.¹² Nishizuka *et al.*¹³ have demonstrated the growth of semipolar $\{11\bar{2}2\}$ InGaN quantum wells on the sidewalls of patterned *c*-plane oriented stripes. In this work, we demonstrate a green InGaN/GaN LED on a planar semipolar ($10\bar{1}\bar{3}$) GaN template.

The semipolar green InGaN/GaN LED structure was grown by metalorganic chemical vapor deposition in a horizontal-flow reactor, on a 20- μ m-thick specular and optically transparent semipolar ($10\bar{1}\bar{3}$) GaN template on *m* sapphire grown by hydride vapor phase epitaxy (HVPE). Analysis of the HVPE-grown template using transmission electron microscopy yielded a defect structure dominated by basal plane stacking faults and threading dislocations in the $\langle 10\bar{1}0 \rangle$ directions on the (0001) plane. Convergent beam electron diffraction of the HVPE-grown template revealed that the negative *c* direction emerged from the surface of the ($10\bar{1}\bar{3}$)

^{a)} Author to whom correspondence should be addressed; electronic mail: rajat@engineering.ucsb.edu

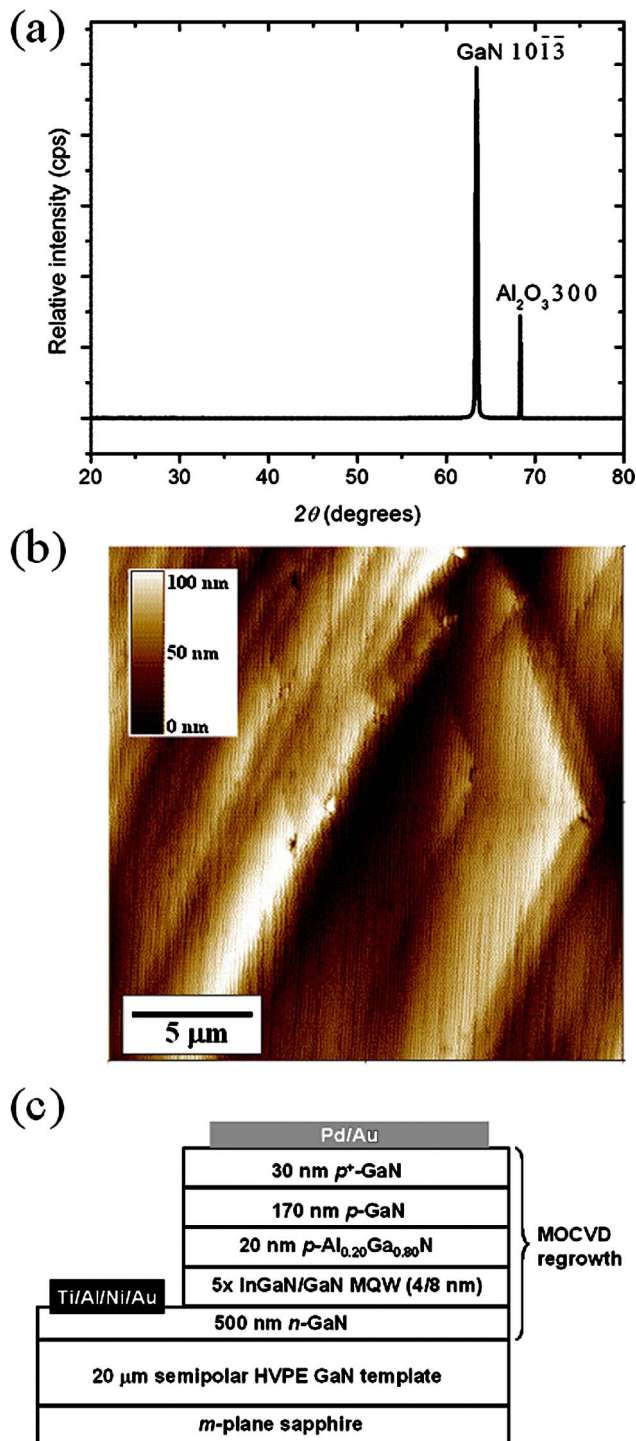


FIG. 1. (a) A 2θ - ω x-ray scan indicating the surface orientation of the GaN ($10\bar{1}3$) film on *m* sapphire. (b) AFM image of the ($10\bar{1}3$) GaN film surface. (c) Schematic of the semipolar green LED.

film. Figure 1(a) shows an on-axis x-ray diffraction scan for the HVPE-grown template, confirming the ($10\bar{1}3$) surface orientation. Figure 1(b) shows an atomic force microscope (AFM) image of the ($10\bar{1}3$) GaN surface over a $20 \times 20 \mu\text{m}^2$ area. Details of the HVPE growth and material characterization will be reported elsewhere.¹⁴ A detailed schematic of the device structure is shown in Fig. 1(c).

Following the growth, a Cl_2 -based reactive ion etch was used to define $300 \times 300 \mu\text{m}^2$ mesas. Ti/Al/Ni/Au (20/50/20/300 nm) and Pd/Au (5/6 nm) were used as the

n-GaN and transparent *p*-GaN contacts, respectively. The fabricated devices were tested on wafer, and all measurements were carried out at room temperature. Details of the test setup are provided elsewhere.⁶

The solid line in Fig. 2(a) shows the *I*-*V* curve for a representative semipolar ($10\bar{1}3$) LED. The device exhibits rectifying behavior, with a low turn-on voltage of 3.2 V and a series resistance of 14.3Ω . The dashed line in Fig. 2(a) shows the *I*-*V* curve for a commercially available green *c*-plane LED (emission at ~ 525 nm) that was used as a reference. The commercial green LED has a turn-on voltage of 3.5 V, and a series resistance of 28.9Ω . The difference in the turn-on voltage between the two LEDs may be attributed to a decrease in the polarization-induced electric fields in the semipolar LED compared to the commercial LED, which should allow current flow across the semipolar diode at lower bias voltages.

Figure 2(b) shows the direct current (dc) electroluminescence (EL) spectra for a representative semipolar LED for various drive currents in the range 20–250 mA. The peak emission wavelength blueshifts from 527.1 nm at 20 mA to 520.4 nm at 250 mA, representing a net shift of 6.7 nm over a 230 mA range. The inset in Fig. 2(b) shows the peak emission wavelength as a function of drive current for both the semipolar green LED and the commercial green LED. The commercial green LED shows a shift in emission from 522.4 nm at 20 mA to 510 nm at 100 mA, representing a net shift of 12 nm over an 80 mA range. We attribute the reduced blueshift in the semipolar green LED with increasing drive current to reduced polarization-induced electric fields in the active region of the device compared to the commercial *c*-plane LED. Additionally, based on preliminary calculations, we believe that the appearance of a shoulder at ~ 450 nm in the EL emission spectra at large drive currents is likely related to the population of, and emission from, the $n=2$ level of the InGa_{*x*}N quantum wells.

Figure 2(c) shows the variation of output power and external quantum efficiency (EQE) as a function of drive current for the semipolar green LED. The LED was measured by on-wafer probing, and, consequently, the output power values for the semipolar LED were significantly lower than that for a typical packaged commercial *c*-plane LED. From past measurements, we estimate that the output power for the bare-chip LED should improve by roughly five-fold after packaging. Figure 2(c) shows that the output power for the semipolar green LED increases approximately linearly within the measured range of drive currents of 5–250 mA. A dc output power value of $264 \mu\text{W}$ was measured at a drive current of 250 mA. The EQE was 0.041% at a drive current of 20 mA and increased as the drive current was increased, attaining a maximum value of 0.052% at a drive current of 120 mA, after which it decreased gradually as the drive current was increased. Such a trend in the EQE as a function of drive current is typically observed in long wavelength arsenide- and phosphide-based LEDs. The origin of the atypical variation of EQE with drive current for the semipolar green LED is presently unknown, but we speculate that it is related to the reduced built-in electric fields along the conduction direction of these semipolar nitride LEDs.

Gardner *et al.*⁹ have shown polarization anisotropy in the EL emission for *m*-plane InGa_{*x*}N-GaN LEDs; we observed similar anisotropic emission from the semipolar nitride LEDs. Figure 2(d) shows the EL intensity as a function of

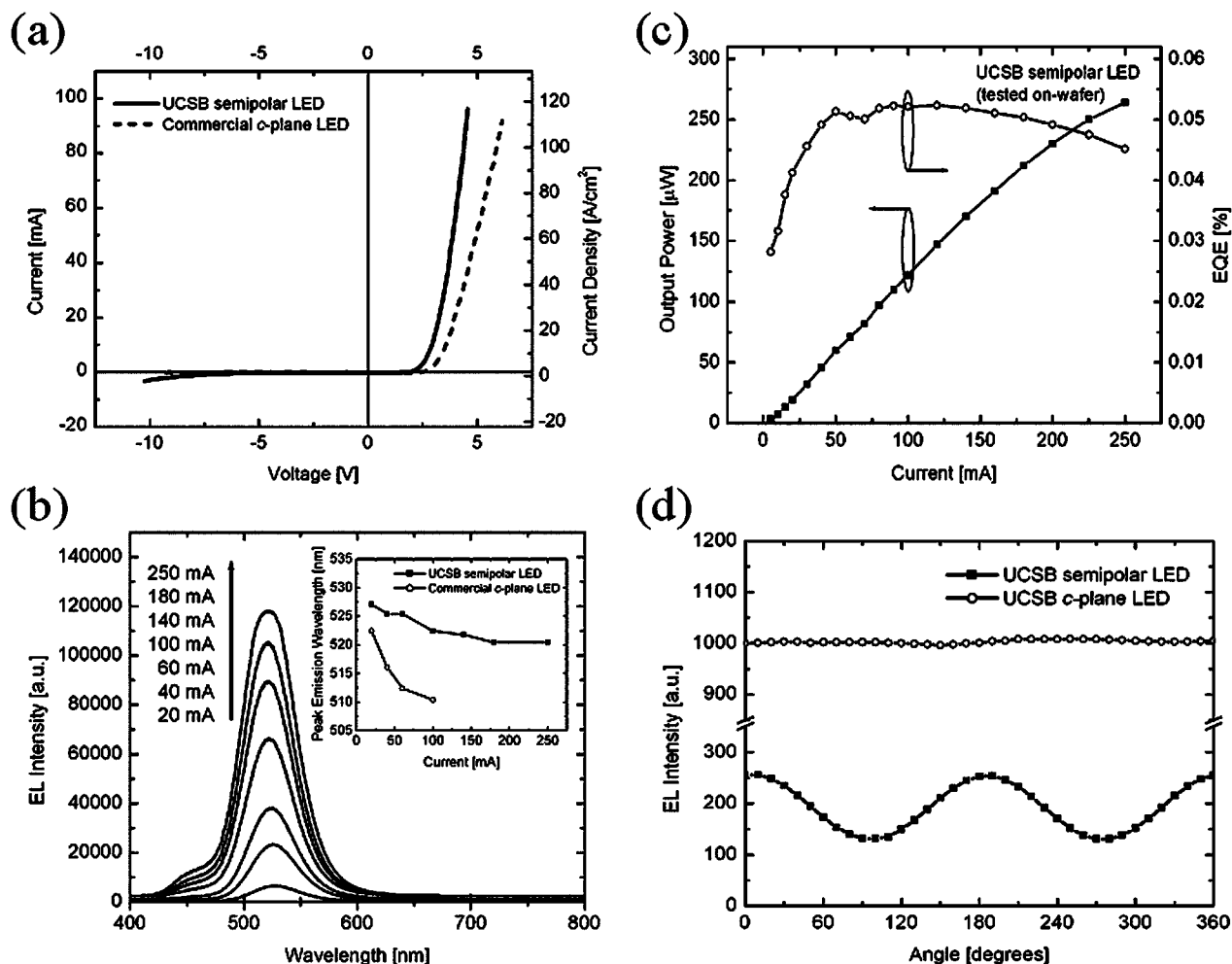


FIG. 2. (a) I - V curves for the semipolar green LED (solid line) and the commercial c -plane green LED (dashed line). (b) EL spectra for the semipolar green LED under varying drive currents. The inset shows the variation of peak emission wavelength as a function of drive current for the semipolar green LED as well as for the commercial c -plane green LED. (c) Output power and EQE as a function of drive current for the semipolar green LED, tested on wafer. (d) Variation of output power with the orientation of a polarizing filter placed between the sample and the Si photodiode, for the semipolar green LED and for an unpackaged c -plane green LED.

the orientation of a polarizing filter placed between the semipolar green LED and the Si photodiode, at a drive current of 20 mA. It can be seen that there is a periodic variation of the EL intensity with angular orientation of the polarizer, with the EL intensity being strongest parallel to the $[1\bar{2}10]$ direction [corresponding to the EL intensity at approximately 0° and 180° in Fig. 2(d)]. This indicates that the light collected from the semipolar LED is partially polarized, and the polarization ratio ρ [defined as $\rho = (I_{\max} - I_{\min}) / (I_{\max} + I_{\min})$] was 0.32 at a drive current of 20 mA. The emission polarization anisotropy is believed to be related to the crystal field along the c axis in wurtzite GaN and the influence of this field on the valence band structure.¹⁵ Corresponding data collected on wafer from a conventional c -plane green LED did not show any evidence of polarization anisotropy.

Ammonia gas was provided by Showa Denko America Inc. This work was funded by the UCSB Solid State Lighting and Display Center and the U.S. Department of Energy. The template growth was funded by the NICP/ERATO JST project. This work made use of the MRL Central Facilities supported by the National Science Foundation under Award No. DMR00-80034.

- ¹T. Takeuchi, S. Sota, M. Katsuragawa, M. Komori, H. Takeuchi, H. Amano, and I. Akasaki, *Jpn. J. Appl. Phys., Part 2* **36**, L382 (1997).
- ²P. Lefebvre, A. Morel, M. Gallart, T. Taliercio, J. Allegre, B. Gil, H. Mathieu, B. Damlano, N. Grandjean, and J. Massies, *Appl. Phys. Lett.* **78**, 1252 (2001).
- ³N. Grandjean, B. Damlano, S. Dalmasso, M. Leroux, M. Laugt, and J. Massies, *J. Appl. Phys.* **86**, 3714 (1999).
- ⁴J. S. Im, H. Kollmer, J. Off, A. Sohmer, F. Scholz, and A. Hangleiter, *Phys. Rev. B* **57**, R9435 (1998).
- ⁵M. Suzuki and T. Uenoyama, *J. Appl. Phys.* **80**, 6868 (1996).
- ⁶A. Chakraborty, B. A. Haskell, S. Keller, J. S. Speck, S. P. DenBaars, S. Nakamura, and U. K. Mishra, *Appl. Phys. Lett.* **85**, 5143 (2004).
- ⁷A. Chakraborty, B. A. Haskell, S. Keller, J. S. Speck, S. P. DenBaars, S. Nakamura, and U. K. Mishra, *Jpn. J. Appl. Phys., Part 2* **44**, L173 (2005).
- ⁸A. Chitnis, C. Chen, V. Adivarahan, M. Shatalov, E. Kuokstis, V. Mandavilli, J. Yang, and M. A. Khan, *Appl. Phys. Lett.* **84**, 3663 (2004).
- ⁹N. F. Gardner, J. C. Kim, J. J. Wierer, Y. C. Shen, and M. R. Krames, *Appl. Phys. Lett.* **86**, 111101 (2005).
- ¹⁰S. H. Park, *J. Appl. Phys.* **91**, 9904 (2002).
- ¹¹M. McLaurin, T. E. Mates, and J. S. Speck, *Appl. Phys. Lett.* **86**, 262104 (2005).
- ¹²S. H. Park and S. L. Chuang, *Phys. Rev. B* **59**, 4725 (1999).
- ¹³K. Nishizuka, M. Funato, Y. Kawakami, S. Fujita, Y. Narukawa, and T. Mukai, *Appl. Phys. Lett.* **85**, 3122 (2004).
- ¹⁴T. J. Baker, B. A. Haskell, F. Wu, P. T. Fini, J. S. Speck, and S. Nakamura (unpublished).
- ¹⁵K. Domen, K. Horino, A. Kuramata, and T. Tanahashi, *Appl. Phys. Lett.* **71**, 1996 (1997).